ISSN: 2723-9535

Available online at www.HighTechJournal.org

HighTech and Innovation Journal

Vol. 7, No. 2, June, 2026

Lacquerware Color and Pattern Design Method Based on Improved Clustering and Edge Detection

Wei Pan [1], Bo Hong [2*]

[1] School of Textile Garment and Design, Suzhou University of Technology, Suzhou 215500, China.

[2] School of History, Nanjing University, Nanjing 210023, China.

Received 02 September 2025; Revised 22 April 2026; Accepted 05 May 2026; Published 01 June 2026

Abstract

To realize accurate extraction and digital design of lacquerware color and decorative patterns for traditional craft inheritance and innovation, this study proposes an improved technical method. The improved K-means++ clustering algorithm is used for color extraction. First, singular value decomposition (SVD) reduces the dimensionality of compressed images to retain core color information. Then, a quadratic clustering strategy optimizes the initial centers. For pattern detection, hybrid adaptive median filtering and bootstrap filtering denoise images, combined with adaptive linear interpolation suppression, improve edge positioning accuracy. Experiments on typical lacquerware images showed that when extracting 16 feature colors, the improved K-means++ had a mean peak signal-to-noise ratio (PSNR) of 31.47 dB and a structural similarity index (SSIM) of 0.95. When extracting 8 colors, it still maintained a PSNR of 28.83 dB. The improved Canny algorithm achieved a PSNR of 24.43 dB at 1.0% noise level, with 64.88% sensitivity and 93.04% specificity. It accurately restored color proportions of crafts like needle carving with a pulling knife and generates patterns with clear edges. This method synergistically optimizes color and edge extraction, enhances digital design precision and efficiency, and provides reliable support for traditional craft digital preservation.

Keywords: K-means++; Edge Detection; Color Clustering; Tattoo Design; Bootstrap Filtering.

1. Introduction

In Chinese traditional culture, lacquerware occupies a pivotal position with its unique artistic charm and exquisite craftsmanship. From the gorgeous decorations of ancient royal palaces to the exquisite objects of daily life, lacquerware not only carries a deep historical and cultural heritage, but also reflects the exquisite skills of craftsmen. The use of color and decorative pattern is the soul of lacquerware art. The interplay of the two gives lacquerware a high artistic value and ornamental value. Nowadays, in the context of the digital era, how to achieve the innovative development of lacquerware color and decorative pattern design with the help of advanced technical means has become a key topic of cultural heritage and craft revitalization [1]. The traditional lacquerware production process is complex and has a long cycle, and the creation of colors and decorative patterns relies on the personal experience and inspiration of the craftsmen. Therefore, there are many limitations in this way: the color extraction is not precise enough, and it is difficult to meet the standardized demand of mass production. The decorative pattern design is inefficient and cannot respond quickly to market changes. Manual operation is easily disturbed by environmental factors, resulting in unstable product quality [2].

* Corresponding author: 602024100003@smail.nju.edu.cn

https://doi.org/10.28991/HIJ-2026-07-02-020

➢ This is an open access article under the CC-BY license (https://creativecommons.org/licenses/by/4.0/).

© Authors retain all copyrights.

Clustering algorithms and pattern edge detection approaches have produced impressive results in the field of image processing in recent years due to the rapid advancement of computer vision technology. This provides a new opportunity for the digital transformation of traditional lacquerware craft. Research in the field of digital design has begun to explore topics such as achieving color extraction through image segmentation algorithms and applying edge detection technology to enhance the accuracy of pattern recognition. However, existing methods often struggle to accurately separate the proportion relationship between the base color and accent color when dealing with the problem of multi-process color fusion. These methods are also insufficient for handling issues of multi-process color fusion and noise sensitivity. In terms of edge detection, deficiencies remain in retaining weak edges and in adaptive threshold processing. These deficiencies result in an inability to effectively capture subtle changes in object patterns. Furthermore, the lack of a collaborative optimization design method tailored to the characteristics of lacquerware craftsmanship makes it difficult to achieve precise digital expression of colors and patterns [3-5]. In response to the above research gaps, this study proposes a digital design method for the color and pattern of lacquerware based on improved K-Means ++ clustering and Canny edge detection. In terms of color extraction, singular value decomposition (SVD) reduces the dimension, compresses the image, and retains the core color information. It also combines a secondary clustering strategy to optimize the initial center sensitivity problem. In terms of pattern detection, a hybrid filtering denoising method that combines adaptive median filtering and guided filtering is used. Additionally, adaptive linear interpolation is employed to improve the accuracy of edge positioning, thereby enhancing the precision and efficiency of the digital design process for lacquerware.

The innovative aspect of the research is the proposed image dimensionality reduction and compression strategy based on SVD and a secondary clustering optimization method. The first round adaptively generates the main color set, and the second round fuses them to generate the core main colors. This approach addresses the issue of initial center sensitivity in color extraction, which is characteristic of lacquerware craftsmanship. In the detection of patterns, an innovative hybrid filtering denoising mechanism is formed by integrating adaptive median filtering and guided filtering, and adaptive linear interpolation is introduced to improve the edge positioning accuracy. Among them, adaptive median filtering and guided filtering are existing technologies, but their collaborative optimization and targeted improvement are the innovations of this study. The research contributes to enhancing the accuracy of color extraction and the integrity of decorative edges on lacquerware. It provides a reliable technical path for digitizing and standardizing the design of lacquerware craftsmanship. The research effectively promotes the deep integration and application of traditional craftsmanship and modern digital technology.

The technical path and content framework structure of the research are as follows: First, systematically sort the existing research results on color extraction and edge detection in the "Related Works" section. Then, further clarify the differences between this research and existing work, as well as the innovative entry points. The "Methods and Materials" section elaborates on the improvements to the two core technologies, including the K-Means++ color extraction algorithm, which is based on SVD dimensionality reduction and secondary clustering, as well as the Canny edge detection algorithm, which is based on hybrid filtering and adaptive linear interpolation suppression. Subsequently, in the "Results" section, the hardware platform, software environment, and lacquerware image samples used in the experiment are described. Through comparative experiments, the improved algorithm's performance advantages in color extraction and edge detection are verified, as well as its application effects in typical lacquerware techniques, such as knife-needling and silver-silk-gloss engraving. The "Discussion" section analyzes the core advantages of the improvement methods, the limitations of the current research, and the future optimization directions. Finally, the "Conclusion" section summarizes the technical contributions of this research and clarifies the value of this method in preserving lacquerware craftsmanship and its potential application to other cultural relics, such as ceramics, weaving, and embroidery.

2. Related Works

The extraction and analysis of color features have important applications in many fields such as image segmentation and cultural heritage research. Related scholars have carried out many explorations around this topic. To achieve color image segmentation based on color features, Bhagat et al. extracted image colors through a three-stage operation of preprocessing (filtering images by Wiener filter model), feature extraction (shape index histogram, improved local gradient pattern, color features), and segmentation (improved kernel fuzzy C-means (FCM) algorithm combined with self-improved snake optimization algorithm for selecting the best quality centers). According to the findings, the suggested approach performed better than the current models in terms of specificity, accuracy, and other metrics [6]. Ning et al. employed a combined technique of adaptive gamma correction and KMC segmentation to address the issue of missing features brought on by uneven illumination in the texture extraction of Tenglong Yuanqinghua. The method enhanced the texture by gray scale transformation to adjust the brightness, Gaussian filtering, weighted average multi-

scale convolution, and 2D gamma correction. Moreover, it combined with Lab space KMC segmentation. The method's segmentation accuracy was 95%, according to the results, which might significantly increase the texture extraction accuracy [7].

To identify copper corrosion grades quickly, Qian et al. reduced the dimensionality by image segmentation, filter processing, color quantization, and kernel principal component analysis. The method was combined with semi-supervised KMC, and the model was trained with standard colorimetric card color feature vectors as the initial clustering center. The results indicated that the classification results of the algorithm matched well with the visual inspection results with high accuracy [8]. To characterize the color of small ochre samples, Anisovets et al. used a stereomicroscope and a Menzel soil color card for visual color determination. The method converted the Menzel values to CIE Lab* coordinates and then performed cluster analysis and principal component analysis. The outcomes revealed that the technique was able to recognize characteristic relationships of cultural layer structures, reliably identify a wide range of artistic practices, and potentially serve as a chronological marker for multilayered sites [9].

Edge detection and pattern extraction are the key links in pattern analysis and reconstruction of cultural relic images. Aiming at the shortcomings of traditional algorithms, researchers have carried out a series of improvements and optimizations. Zhang et al. solved the problems of manually determining the threshold value and low extraction efficiency of traditional Canny operator in order to realize the automatic extraction of texture pattern of embroidered cultural relics images. The method adopted genetic algorithm to solve the Canny optimal threshold for edge detection, smoothed the image by bilateral filtering and mean drift algorithm, and filtered the noise by using morphological expansion and connectivity domain area. The results indicated that the algorithm pattern extraction accuracy and pixel accuracy were better than the traditional method [10]. To increase the precision and practicality of acquiring and converting 2D paper sample contour information, Tuo et al. introduced new 45° and 135° directional gradient templates based on the CA. The method adopted adaptive bilateral filtering to replace the traditional Gaussian filtering, and introduced an adaptive dual threshold selection mechanism to determine the edge threshold dynamically. The results indicated that the method had an extraction error of 0.15 cm to 1.50 cm, which was in line with the clothing standard [11].

To study ancient textile patterns and realize intelligent understanding and automatic design using computer vision technology, Shi et al. constructed a Tang Dynasty regimental areal pattern dataset and conducted qualitative and quantitative experiments by proposing a perceptually consistent contour extraction method that simulates the retina, lateral geniculate body and primary visual cortex. According to the findings, the technique could efficiently recover contours, suppress minute pixel shifts, and improve edge information. It was also shown that the cortical simulation was directionally selective [12]. Yadav et al. aimed to propose low-dimensional edge descriptors for medical images using a method based on local diagonal and non-diagonal maximum-minimum patterns. This method utilized intermediate pixel localization relations to reduce feature vector lengths while maintaining edge map quality. When compared to a number of different approaches, the results demonstrated that the method performed better than the state-of-the-art in terms of accuracy and Jaccard similarity index [13].

In summary, the existing studies use clustering algorithms in color extraction to enhance image segmentation accuracy, but insufficiently deal with multi-process color fusion and noise sensitivity of lacquerware. Edge detection enhances the integrity of pattern extraction by optimizing the Canny operator, but still lacks in weak edge retention and adaptive thresholding. Therefore, this study proposes an improved K-means++ algorithm that combines SVD downscaling and quadratic clustering to optimize color extraction. It also designs hybrid filtering and adaptive interpolation to enhance the robustness of color reproduction and edge detection in lacquerware decorative pattern design using the improved CA.

3. Material and Methods

3.1. Lacquerware Color Extraction Based on Improved K-means++

In lacquerware color and decorative pattern design, the core objective of the clustering algorithm is to extract representative colors from complex decorative pattern features. A clearer data distribution and higher computation speed allow the standard KM++CA to achieve a superior clustering impact. Clustering bias can easily result from its sensitivity to the original center, noise, and outliers [14, 15]. The study uses SVD to compress the image before the clustering algorithm selects the first center letter in order to solve this issue. By filtering the pixels with high and large percentage of retained information, the image information can be maximally retained while the number of pixels is significantly reduced, thus improving the color extraction accuracy. The processing of SVD is shown in Figure 1.

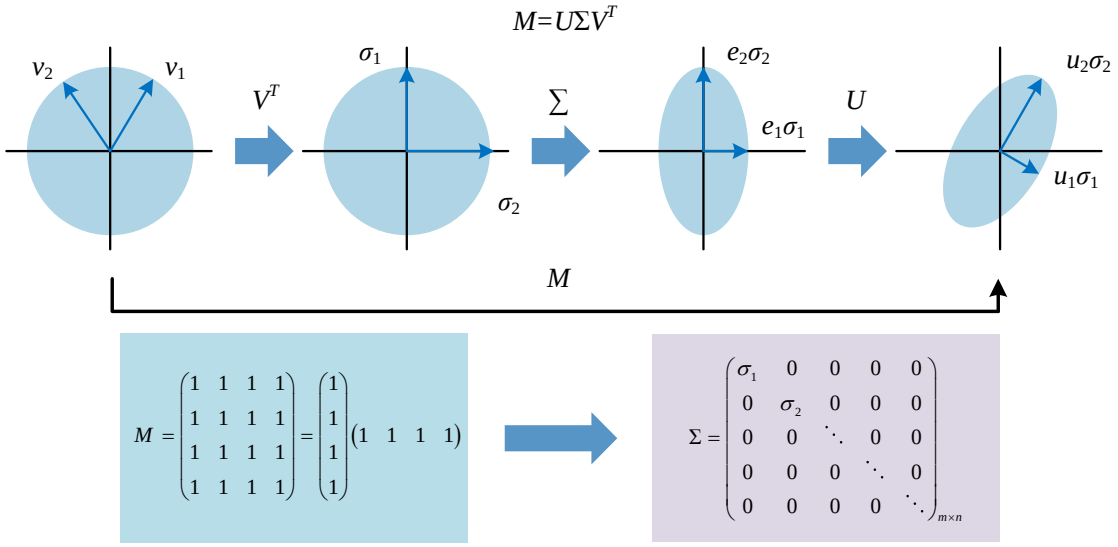

Figure 1. Processing process of SVD

Figure 1 illustrates the two-dimensional linear transformation process of SVD. The core idea is to decompose an arbitrary matrix M into the product of three matrices as shown in Equation 1.

$$M = U\Sigma V^T \tag{1}$$

In Equation 1, U, $\sum$, and V^T are the left singular, diagonal, and right singular matrix, respectively. T is the transpose of matrix V. The left side is the unit circle in the original space on which standard orthogonal basis vectors, such as v_1 and v_2, are uniformly distributed. The orthogonal matrix V^T rotates the original coordinate system to the direction corresponding to the diagonal matrix $\sum$. $\sum$ scales the ellipse along the direction of the coordinate axes. U rotates the transformed elliptic coordinate system to the standard direction. In the middle, a linear transformation of the unit circle is performed by the matrix M to obtain the ellipse on the right side. The long and short axes of the ellipse correspond to the transformed orthogonal basis vectors (e.g., u_1 and u_2), whose lengths are determined by the singular values σ_1 and σ_2, respectively. In the image matrix, SS is computed as shown in Equation 2.

$$M = \sigma_1 u_1 v_1^T + \sigma_2 u_2 v_2^T + \cdots \sigma_b u_b v_b^T \tag{2}$$

In Equation 2, n is the ordinal index of the singular values. SVD achieves denoising and dimensionality reduction through the energy concentration of singular values. The main information of the matrix is concentrated in a few large singular values. For dimensionality reduction, the first b large singular values and the columns and rows corresponding to U and V^T are retained, and the original matrix is reconstructed with low-order submatrices to realize dimensionality compression. For denoising, the small singular values are truncated and only the large singular values are used to reconstruct the image, filtering out the noise component while retaining the core features [16, 17]. After compressing the image using SVD, the study further extracts the color by quadratic clustering. The extraction process is shown in Figure 2.

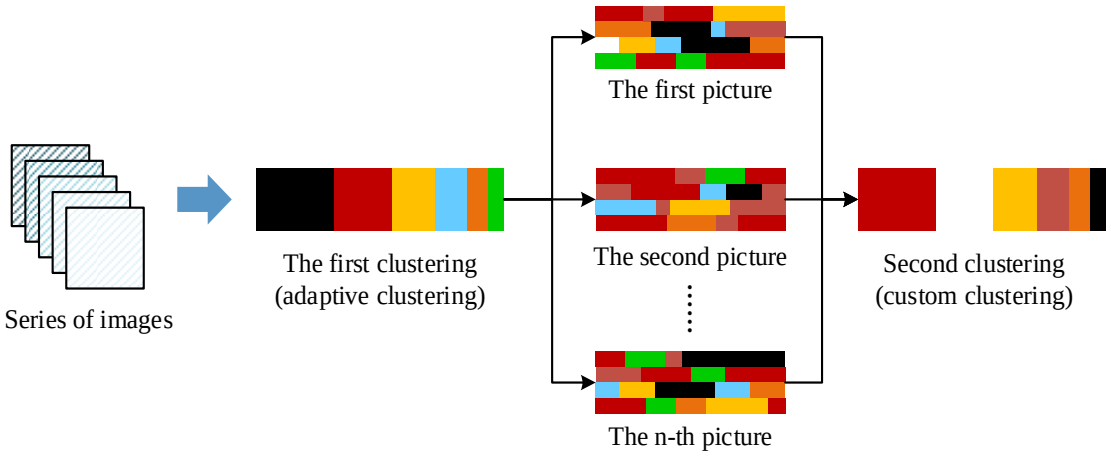

Figure 2. Secondary clustering color extraction process

In Figure 2, for a sample set containing n lacquerware images, the study first generates a set of primary colors with number K1 for each image independently using adaptive clustering. After that, the first round of primary color results of all images are integrated as input samples to implement secondary custom clustering. Ultimately, K2 core primary colors characterizing the comprehensive color features of the series of images are generated. The value of K2 can be set manually based on design requirements or on the number of color-matching areas in the pattern artwork. This allows for the fusion of color features for design applications. In the first clustering, the set of clustered sample points $\{a_1, a_2, \ldots, a_n\}$ is the pixel points of the input image. The study measures the similarity of the two sample points by Euclidean distance and designs the critical distance L as a classification criterion between the sample points. Equation 3 provides the calculation of the critical distance [18].

$$L = \frac{2\sum_{i=1}^{n}\sum_{j=i+1}^{n} l(i, j)}{n(n-1)} \tag{3}$$

In Equation 3, l displays the Euclidean distance between sample points a_i and a_j. n is the total number of pixel sample points in the input image. The adaptive clustering method for the first clustering is shown in Figure 3.

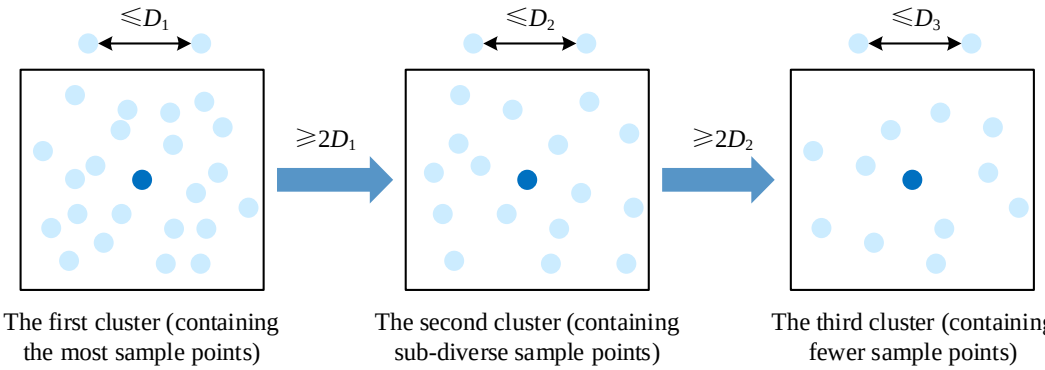

Figure 3. Adaptive clustering method

In Figure 3, each data point is used as the center to classify and count the number of points in the cluster based on the critical distance L. The center of mass (COM) of the largest cluster is selected as the initial clustering center. If the Euclidean distance between the COM of the second largest cluster and the initial center exceeds $2L$, it is established as the secondary center. Iterative screening is performed according to this criterion so as to determine the final set and quantity of clustering centers. The secondary clustering takes the first clustering results as sample points and sets the initial number of cluster centers by hand. The Euclidean distance from the non-center sample points to each center is calculated and grouped into the nearest cluster class. Then the COM coordinates of each cluster are recalculated as the new clustering center. The sample assignment and COM update operations are repeated until the cluster centers remain unchanged. Finally, a comprehensive master chromatogram characterizing the color features of the series of images is obtained. After that, based on the results of color feature extraction, a color network relationship model is established to provide color information reference for lacquerware color matching. The connecting line between colors reflects the co-occurrence relationship of the paired colors, and the thickness of the connecting line is determined by the co-occurrence rate $\rho_{i,j}$. Equation 4 illustrates how $\rho_{i,j}$ is calculated.

$$\rho_{i,j} = \sum_{r=1}^{A} a_r \Big/ A \tag{4}$$

In Equation 4, A is the total number of images. a_r denotes the co-occurrence of the extracted colors i and j in the rth image. The extracted colors are presented as circles of the corresponding color, with the size of the circle determined by its percentage. Each color circle is arranged in a circular pattern. The amount of retrieved colors corresponds to the image's true color condition based on the clustering algorithm suggested in the study. After that, the extracted colors are rearranged in descending order and in counterclockwise rings to facilitate the visual judgment of the amount of color used. The Euclidean distance between colors is marked on the connecting lines of co-occurring colors. The number of connecting lines is reduced by setting a co-occurrence rate threshold, which improves the ability to judge color correlation and provides clearer reference information for color design. The inter-color Euclidean distance $H_{i,j}$ is calculated as shown in Equation 5 [19].

$$H_{i,j} = \sqrt{\left(R_i - R_j\right)^2 + \left(G_i - G_j\right)^2 + \left(B_i - B_j\right)^2)} \tag{5}$$

In Equation 5, R_i and R_j, G_i and G_j, and B_i and B_j are the red, green, and blue color values of the ith and jth extracted colors, respectively. The flow of color extraction algorithm of lacquerware based on improved K-means++ is shown in Figure 4.

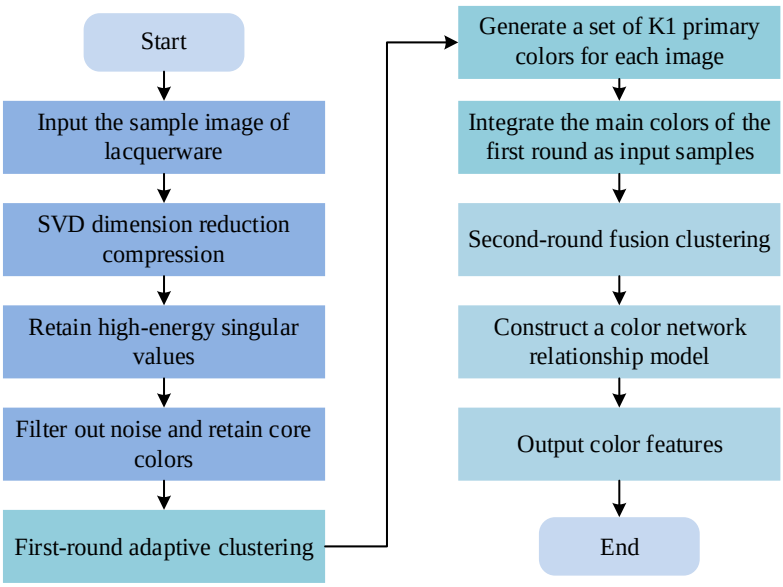

Figure 4. The color extraction algorithm process of lacquerware based on the improved K-Means ++

Figure 4 shows the improved K-means++ color extraction algorithm process. First, a sample set of lacquerware images is input and compressed by SVD for dimensionality reduction. Then, high-energy singular values are retained to filter out noise and maximize preservation of core color information. Then, the first round of adaptive clustering is performed on the pixels of the compressed image. This process dynamically generates a set of K_1 dominant colors for each image based on the critical distance. This realizes the initial extraction of the dominant colors of a single image. Next, the primary colors of all the images from the first round are integrated as input samples for the second round of fusion clustering. This generated the K_2 core primary colors, which characterize the comprehensive color features of the image series. Finally, a circular color network model is constructed based on the proportion and co-occurrence of the core primary colors. The size of the circle reflects the proportion of each color, the thickness of the connecting lines reflects the co-occurrence rate, and the distance between colors visually displays their proportion and strength of association. This model provides a clear, quantitative reference for lacquerware color design.

3.2. Lacquerware Decorative Pattern Edge Detection Based on Improved CA

On the basis of obtaining the core color characteristics of lacquerware by improving the K-means++ algorithm, decorative pattern, as another key carrier of lacquerware artistic expression, the clarity and completeness of its edge contour directly determine the accuracy of pattern reconstruction. The CA is one of the commonly used algorithms in image edge detection, which removes the noise interference in the image through Gaussian filter to reduce the false detection. Since the Gaussian filter in the traditional CA only achieves smoothing through spatial neighborhood distance weighting, it leads to a significant attenuation of weak edge information in the filtering process. Meanwhile, its suppression effect on pepper noise is limited, and the filtering performance is highly dependent on the artificially set standard deviation parameter [20, 21]. To address this problem, the study designs a hybrid filtering algorithm to process lacquerware images. The image is first denoised using adaptive median filtering, which decides whether to resize the window or replace the pixel value (PV) through a two-stage judgment. In stage 1, if the median value z_{med} of the current window is neither the minimum nor the maximum, the median value is probable to be a valid pixel, which can be used to determine whether the center pixel is noise. The judgment condition is shown in Equation 6.

$$\begin{cases} Z_1 = z_{med} - z_{\min} \\ Z_2 = z_{med} - z_{\max} \end{cases} \tag{6}$$

In Equation 6, z_{min} and z_{max} are the minimum and maximum values of the pixels in the window, respectively. Z_1 and Z_2 are the difference between the median value and z_{min} and z_{max}, respectively. When $Z_1 > 0$ and $Z_2 < 0$, the 2-stage is entered. If it is not satisfied, the window size is large. If the maximum window size is not exceeded then repeat stage 1, otherwise output z_{med}. The judgment condition of stage 2 is shown in Equation 7.

$$\begin{cases} Z_3 = z_{xy} - z_{\min} \\ Z_4 = z_{xy} - z_{\max} \end{cases} \tag{7}$$

In Equation 7, z_{xy} is the gray value of the pixel at the center of the current filter window. Z_1 and Z_2 are the difference between z_{xy} and z_{min} and z_{max}, respectively. If $Z_3 > 0$ and $Z_4 < 0$, output z_{xy}, otherwise output z_{med}. This process preserves edge details while removing noise by dynamically adjusting the window size [22, 23]. After that, the filtering result is used as an input to the bootstrap filter to preserve more edge details. The core mechanism that distinguishes the bootstrap filter from conventional filters is the introduction of a bootstrap image as an a priori constraint. This picture could be any external image or the input image itself. The filter dynamically generates transmission coefficients by parsing the local structural features of the bootstrap image. This process couples the content semantics of the bootstrap image with the statistical characteristics of the input image, thereby achieving semantics-driven adaptive filtering [24-26]. To further improve the bootstrap filter's edge protection ability, the study proposes a gradient-domain weighted bootstrap filtering method. This method introduces a dual mechanism of edge-aware and edge-protection constraints to accurately recognize and protect the edge structure. Figure 5 illustrates the method's processing flow.

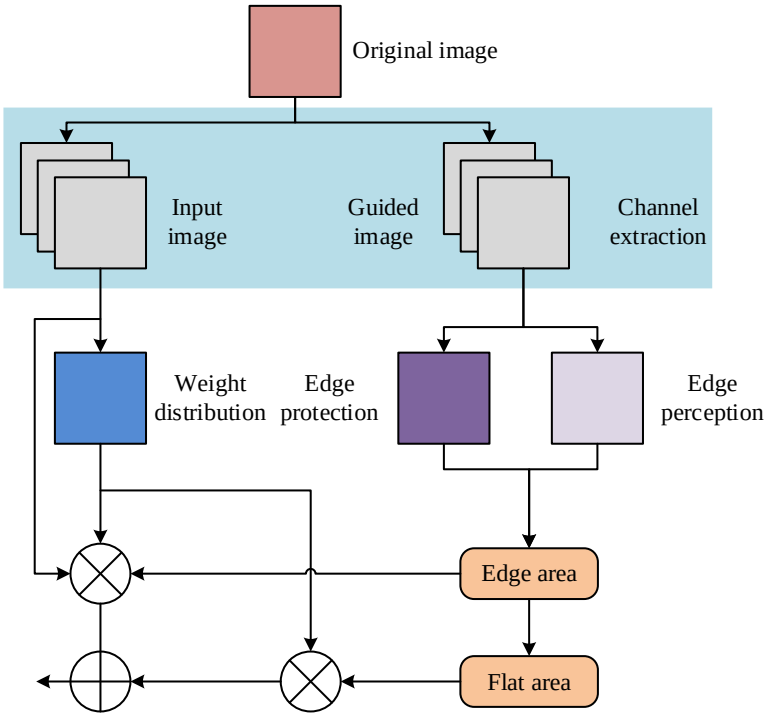

Figure 5. Gradient domain weighted guided filtering process

As shown in Figure 5, the input image first undergoes channel extraction, followed by edge perception to distinguish between edge and flat regions. Then, edge protection processing is applied, combined with the weight distribution of the bootstrap image. These steps constitute the complete gradient-domain weighted bootstrap filtering process. In the edge perception constraint, an adaptive weighting model based on the coefficient of variation of gradient information is proposed. The model dynamically adjusts the filtering intensity by calculating the gradient variation coefficient $\varphi(p')$ of the pixel points within a 3×3 window, as shown in Equation 8.

$$\varphi(p') = \frac{1}{N} \sum \frac{\upsilon(p') + \chi}{\upsilon(p) + \chi} \tag{8}$$

In Equation 8, p displays the center pixel of the window. p' displays any pixel point within the window. N displays the total number of pixels within the window. $\upsilon(\cdot)$ displays a combination of the fused pixel coefficient of variation and the gradient coefficient of variation. χ displays a very small constant used to avoid the denominator being zero. The gradient calculation uses global difference operations in four directions to avoid the complexity of traditional template operations. In the specific implementation, the coefficient of variation $C_V = \theta_d / \mu_d$ is introduced to quantify the degree of dispersion of the gradient distribution by calculating the gradient magnitude in each direction. θ_d and μ_d are the gradient standard deviation and mean, respectively. The pixel point variation coefficient is then measured by the local gray scale variance θ_{p^2}, and finally $\upsilon(p') = C_V \times \theta_{p^2}$. In the edge protection constraint, the coefficient $\upsilon(p') = C_V \times \theta_{p^2}$ in the linear regression model is corrected by introducing the first order edge protection operator ϑ. The corrected formula is shown in Equation 9.

$$a_{p'} = \frac{\sum_{p' \in \omega_p} \varphi(p') \cdot (I(p') - \mu_I) \cdot (P(p') - \mu_P)}{\sum_{p' \in \omega_p} \varphi(p') \cdot (I(p') - \mu_I)^2 + \eta\zeta} \tag{9}$$

In Equation 9, ω_p denotes the local window centered at p. $I(p')$ and $P(p')$ display the PVs of the guiding image and the input image at p', respectively. μ_I and μ_P are the pixel mean values of the guide image and input image in the window, respectively. η is the edge protection operator, $\eta = 1$ (edge region) when the gradient is greater than 1.7 times the mean value, otherwise $\eta = 0$ (flat region). ζ is the regularization parameter, which is used to balance the model stability with the edge preservation effect. The final optimization model combines the edge-aware weights $\varphi(p')$ with the edge-preserving operator η to obtain a double-constrained linear regression model as shown in Equation 10.

$$\min_{a_p, b_p} \sum_{p' \in \omega_p} \varphi(p') \cdot \left[P(p') - \left(a_p I(p') + h_p \right) \right]^2 + \eta \cdot \zeta \cdot a_p^{\,2} \tag{10}$$

In Equation 10, h_p is the coefficient of the linear model. The model solves a_p and h_p iteratively so as to achieve detail preservation in edge regions with effective smoothing in flat regions. Additionally, the traditional Canny edge detection algorithm selects isotropic neighbor pixels for gradient magnitude comparison based solely on gradient direction during the stage that suppresses extremely large values. Because the selection mechanism homogenizes the pixels involved in the comparison, it relies solely on direction matching. This limitation easily affects the accuracy of edge localization, resulting in reduced reliability of edge determination and connection in subsequent dual-threshold processing [27]. Therefore, the study proposes an adaptive linear interpolation suppression method to achieve pixel-level edge-accurate localization through dynamic interpolation computation. Figure 6 depicts the method's intricate flow.

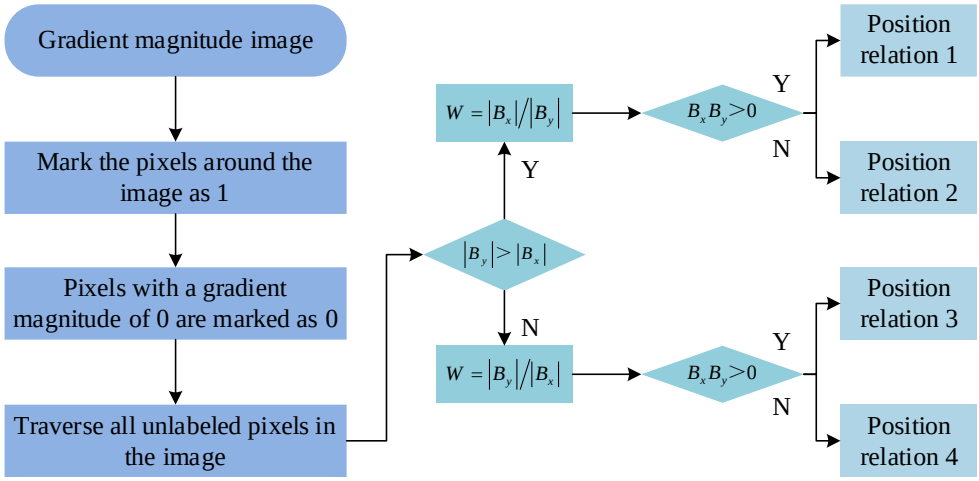

Figure 6. Adaptive linear interpolation suppression method

In Figure 6, since linear interpolation requires global traversal of pixels, and image boundary interpolation requires outward expansion of zero-gradient virtual pixels (whose magnitude formula is smaller than that of neighboring pixels), the pixels on the periphery of the image are marked as 1 (edge candidate). Meanwhile, given that the zero gradient pixel must be a non-edge point, it is directly labeled as 0 in order to reduce the computational redundancy. After the completion of the preprocessing, traversal is performed on the pixels that are not boundaries and have non-zero gradients, and the gradient components B_x and B_y are computed point by point in the directions of x and y. By comparing the modal values of the gradient components, the primary gradient direction can be identified. Moreover, the spatial location of linear interpolation and interpolation weight coefficients are dynamically determined based on the combination of B_x and B_y symbols [28]. The calculation of weight coefficients is shown in Equation 11.

$$\begin{cases} W_1 = |B_x| / |B_y| \\ W_2 = |B_y| / |B_x| \end{cases} \tag{11}$$

In Equation 11, the vertical gradient of the center pixel point is determined to be dominant when $|B_y| > |B_x|$. The weight W_1 is also calculated, and the neighboring pixel position relation is selected based on the sign dissimilarity between B_x and B_y (position relation 1 is used for the same sign, and position relation 2 is used for the same sign). When $|B_y| < |B_x|$, the horizontal gradient of the center pixel point is determined to be dominant. The weight W_2 is also calculated, and the neighbor pattern is selected based on the sign homogeneity as well (position relation 3 is used in case of the same number, and position relation 4 is used in case of the same number). In this case, the position distribution of the neighboring pixel points is shown in Figure 7.

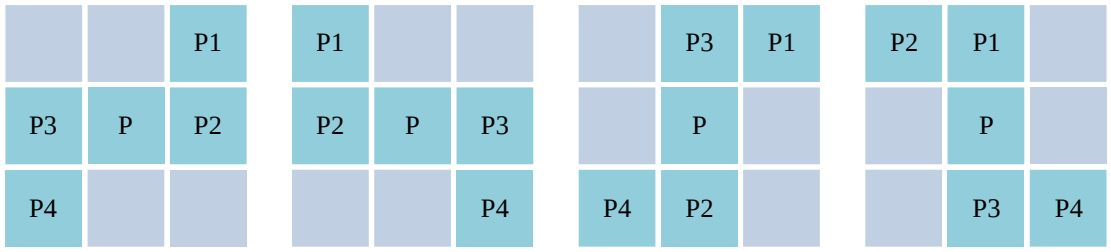

Figure 7. Position distribution of neighboring pixels

In Figure 7, P is the gradient magnitude of the center pixel point. P1 to P4 denote the gradient magnitude of their specific neighborhood pixel points, respectively. These magnitude parameters together construct the local gradient field model [29]. After that, the interpolation calculation is executed based on the above positional relationship, neighborhood pixel gradient magnitude, and weight coefficients, as shown in Equation 12.

$$\begin{cases} M_1 = P_1 \cdot W + P_2 \cdot (1-W) \\ M_2 = P_3 \cdot W + p_4 \cdot (1-W) \end{cases} \tag{12}$$

In Equation 12, M_1 and M_2 are the linear interpolation results calculated from the gradient magnitude of neighboring pixel points P1/P2 and P3/P4 combined with weights, respectively. After edge detection is complete, reconstruction is carried out based on the accurate edge contour. The key points and topology of the edge are extracted, and the inner region of the edge is filled with texture along the gradient direction. This is done by combining the line and pattern unit features of the traditional lacquerware pattern. The filling weights are assigned in proportion to the gradient magnitude by taking the texture of the effective pixels in the neighborhood as a reference. This ensures that the texture near the edge fits the contour, and that the inner region transitions smoothly. Finally, a decorative pattern image that retains the original structure and has coherent details is generated [30].

4. Results

4.1. Validation of Color Extraction Method Based on Improved K-means++

To validate the reliability of the improved K-means++ algorithm in lacquerware color extraction, the study tests and compares the FCM, the original K-means++, and the current advanced color extraction methods [6, 7]. The dataset used in the experiment consists of 240 images of lacquerware. These images are sourced from high-resolution (300 dpi) sketches of lacquerware collected in collaboration between the Shanxi Museum and the Nanjing Museum. The dataset also includes images of modern lacquerware replicas obtained with authorization from the "Exhibition of Traditional Chinese Lacquerware Craftsmanship" (2023, Beijing). The dataset covers six core processes (such as broaching and needle-cutting, silver engraving and silk-reeling, etc.) and eight types of vessel shapes (such as plates, boxes, screens, etc.). The structural similarity index (SSIM) and peak signal-to-noise ratio (PSNR) are used as evaluation indexes. PSNR quantifies the pixel-level error between the reconstructed image and the original image, and its value is positively correlated with the image quality. SSIM, on the other hand, focuses on measuring the fidelity of the structural information of an image by modeling the human visual perception characteristics through three elements: brightness, contrast, and structure. The central processor of the desktop computer used for the experiment is Intel i5-7300HQ, the operating system is Ubuntu 18.04.5 LST, and the software environment is MATLAB R2023a. Table 1 displays the specific parameters of the experimental setup.

Table 1. Parameter information of model training test platform

Hardware facility		Software facility	
Device CPU	Intel i5-7300HQ	Operating system	Ubuntu 18.04.5 LST
Device graphics card	GeForce RTX 2080 Ti	Programming language	Python 3.9
Storage device	SSD 1TB NVMe	Toolkit	CUDA 11.1
Network interface	Gigabit Ethernet	Simulation and testing tools	Jupyter Notebook
Internal memory	16GB DDR4	Programming environment	MATLAB R2023a

The study is carried out to extract the feature colors of the images using each method and the comparison of the image quality obtained by the processing of each method in extracting the 16 feature colors is shown in Figure 8. The PSNR and SSIM comparisons for each image are displayed in Figures 8(a) and 8(b), respectively.

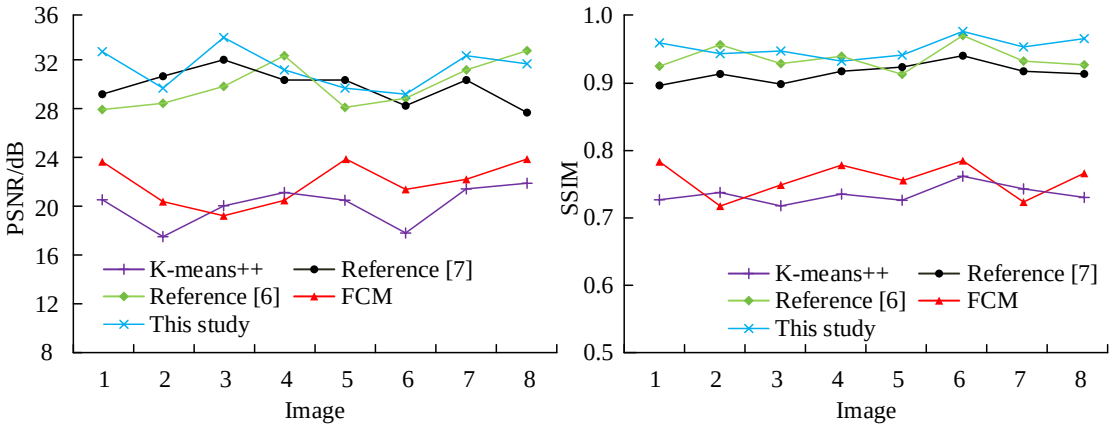

(a) PSNR comparison of images (b) SSIM comparison of images

Figure 8. Comparison of image quality obtained by each method

In Figure 8(a), the PSNR of the proposed improved K-means++ method of the study is slightly lower than that of the Bhagat et al. [6] in image 4 and image 8, and slightly lower than that of the Ning et al. [7] in image 2 and image 5 when extracting 16 feature colors. Its PSNR with images are better than the comparison methods. Images 4 and 8 show lacquerware with a single process and regular color distribution, without the problem of multi-process color fusion. The local optimization strategies for general, regular color images described in Bhagat et al. [6] (e.g., Wiener filtering to suppress single noise and FCM kernel division) can be fully utilized. There is obvious uneven illumination in Images 2 and 5. The adaptive gamma correction in Ning et al. [7] can accurately correct the luminance deviation. The improved K-Means++ focuses on adapting to the multicolored lacquerware, achieving generalization of all types, and optimizing redundancy in these specific scenarios. Therefore, the PSNR is slightly lower. The mean PSNR value of the research method is 31.47dB, while the mean PSNR values of Bhagat et al. [6], Ning et al. [7], FCM, and K-means++ are 30.02dB, 28.37dB, 23.55dB, and 20.06dB, respectively. This indicates that the reconstructed image by this method has less pixel-level error from the original image, and has higher color reproduction accuracy.

In Figure 8(b), the SSIM value of the improved method is also in the leading position, with an average value of 0.95. The research method truncates small singular values and retains high-energy singular values (accounting for more than 95% of the total energy). It filters out weak noise generated by scanning or saving lacquerware images (e.g., unprocessed material reflection noise in Ning et al. [7] study) while compressing the pixel data volume, thus avoiding noise interference with the calculation of cluster centers. In addition, the initial center optimization of the secondary clustering proposed in the research solves the problem of "random initial centers causing cluster offset" in the traditional K-Means ++. For instance, in images of silver-gray inlays on gilded, silk-gloss lacquerware, the traditional K-Means++ algorithm tends to group "silver gray" and "dark gray" together. However, the improved method accurately separates these two low-contrast colors using fine secondary clustering, which increases the PSNR by over 11 dB compared to the original algorithm. In the extraction of eight feature colors, the image quality comparison obtained by the processing of each method is shown in Figure 9. The PSNR and SSIM comparisons for each image are displayed in Figure 9(a) and Figure 9(b), respectively.

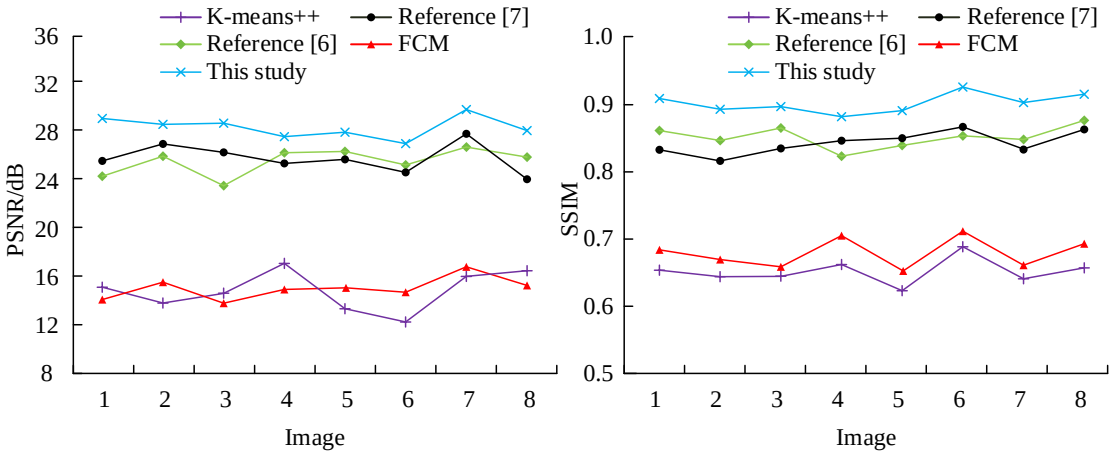

(a) PSNR comparison of images (b) SSIM comparison of images

Figure 9. Comparison of image quality obtained by each method

In Figure 9(a), the overall PSNR of the improved K-means++ method proposed in the study is still better than that of the comparison method when 8 feature colors are extracted, but its mean value decreases compared to that when 16 feature colors are extracted. This is due to the reduction in the number of feature colors. The clustering center's coverage of the complex color distribution in the image is reduced. This results in some subtle color information being simplified, causing an increase in pixel-level error and a lower overall PSNR. Even so, the mean value of PSNR of the research method is 28.83dB, which is still higher than that of Bhagat et al. [6] (25.17dB), Ning et al. [7] (26.31dB), FCM (16.08dB), and K-means++ (15.27dB). It reflects its stability in less feature color extraction. According to Bhagat et al. [6], the kernel FCM algorithm demonstrates that, due to the absence of a priority retention mechanism for core color information, similar colors merge when the number of feature colors decreases, resulting in PSNR. The K-means clustering in Ning et al. [7] do not consider the color proportion correlation of lacquerware craftsmanship (such as the proportion of black base needs to be ≥50%), resulting in a decrease in PSNR.

In Figure 9(b), in the SSIM metric, the average value of the research method is 0.91, which is still higher than the other compared methods. This verifies the ability of the improved algorithm to better balance color simplification and structural fidelity even when the number of feature colors is reduced. The core reason is that SVD dimensionality reduction has already retained the "core color information" of the lacquerware image (such as black base, silver-gray inlay, red-brown accent, and other main colors) in advance. Even if the number of characteristic colors is reduced, the key color components are not lost. However, traditional methods, such as FCM, lose a large number of effective colors immediately after reducing feature colors due to a lack of information screening. This results in a decrease in PSNR.

The study utilizes the improved K-means++ clustering method to extract feature colors for three processes of lacquerware, namely, needle carving with a pulling knife, silver-thread luster carving, and carved flower color filling. The color values and RGB values are directly converted from the pixel channel, and the Lab values are calculated based on the standard RGB conversion formula. Table 2 displays the outcomes of various lacquerware color extraction techniques.

Table 2. Color extraction results of lacquerware by different processes

Craft	Color block	Color value	RGB	Lab	Proportion (%)
Needle carving with a pulling knife		#262425	38/36/37	13.4/0.6/-0.4	66.5
		#4E6127	78/97/39	38.2/-17.8/30.1	12.3
		#3F4448	63/68/72	28.9/-3.2/-2.1	9.2
		#943734	148/55/52	36.2/38.7/21.8	8.5
		#DADEDF	218/222/223	88.1/-1.4/-1.1	3.5
Silver-thread luster carving		#262425	38/36/37	13.4/0.6/-0.4	45.8
		#ACA2A1	172/162/161	67.1/3.4/1.5	22.9
		#66615E	102/97/94	41.4/0.2/4.8	14.3
		#8F361E	143/54/30	35.1/36.3/33.8	10.7
		#873539	135/53/57	34.5/44.2/16.8	6.3
Carved flower color filling		#271815	39/24/21	9.8/5.2/2.8	50.9
		#A01A11	160/26/17	35.6/62.3/44.5	29.1
		#4F5B45	79/91/69	36.8/-15.2/20.3	8.4
		#BE9955	190/153/85	60.5/14.3/41.2	7.2
		#DFB257	223/178/87	70.2/12.5/50.3	4.4

In Table 2, in the process of needle carving with a pulling knife, black primer is used as a base (66.5% of the total), which acts like a canvas for painting. The silver-thread (3.5%) is inlaid into the scoring. Although used in small quantities, its metallic properties create a remarkable glossy contrast and clarity on the black background. The sensitivity of silver-thread to light creates dynamic visual effects in response to changes in ambient light. The dark gray (9.2%) comes from the reflection and absorption effect of silver-thread on the primer, which enhances the three-dimensional sense of the work. Although the proportion of accent colors such as green and red is low, they are effective in enriching the color layers and expressiveness. The silver-thread luster carving process takes black (45.8%) and silver gray (22.9%) as the core characteristic colors. The proportion of the two reaches 68.7%. Black as the base color covers a large area of the surface, while silver gray forms a strong visual contrast with the dark primer through the cool metallic luster, building a multi-layered sense of space. Neutral grey-green (14.3%) in the color space is green-toned tendency, both freshness and stability, assuming the screen color balance function. The total red color accounts for 17%. It serves as the key accent color through the two-tone color system of dark and light, injecting bright vitality into the metal engraving pattern.

4.2. Validation of Edge Extraction Method Based on Improved CA

Eight typical representative lacquerware images are selected as test samples for the experiment, with a uniform resolution of 1024×1024 pixels. To simulate the noise interference in actual preservation, pretzel noise and Gaussian noise with gradient increment from 0.1% to 1.0% are added to the images respectively. In the experiments, the maximum window of the adaptive median filter of the improved CA is set to 7×7, the bootstrap filter regularization parameter σ=0.01, and the double threshold is calculated by Otsu adaptive. The comparison methods are the traditional CA, Laplacian of Gaussian (LOG), and the current advanced research methods [10, 11]. All experiments are tested in the same hardware platform environment. Figure 10 illustrates how the quality of the edge pictures recovered using each technique varies with training in relation to the noise level (NL). Figures 10(a) and Figure 10(b) show the variation of PSNR and SSIM for each image, respectively. Figures 10(c) and Figure 10(d) show the precision and recall variations for each image, respectively.

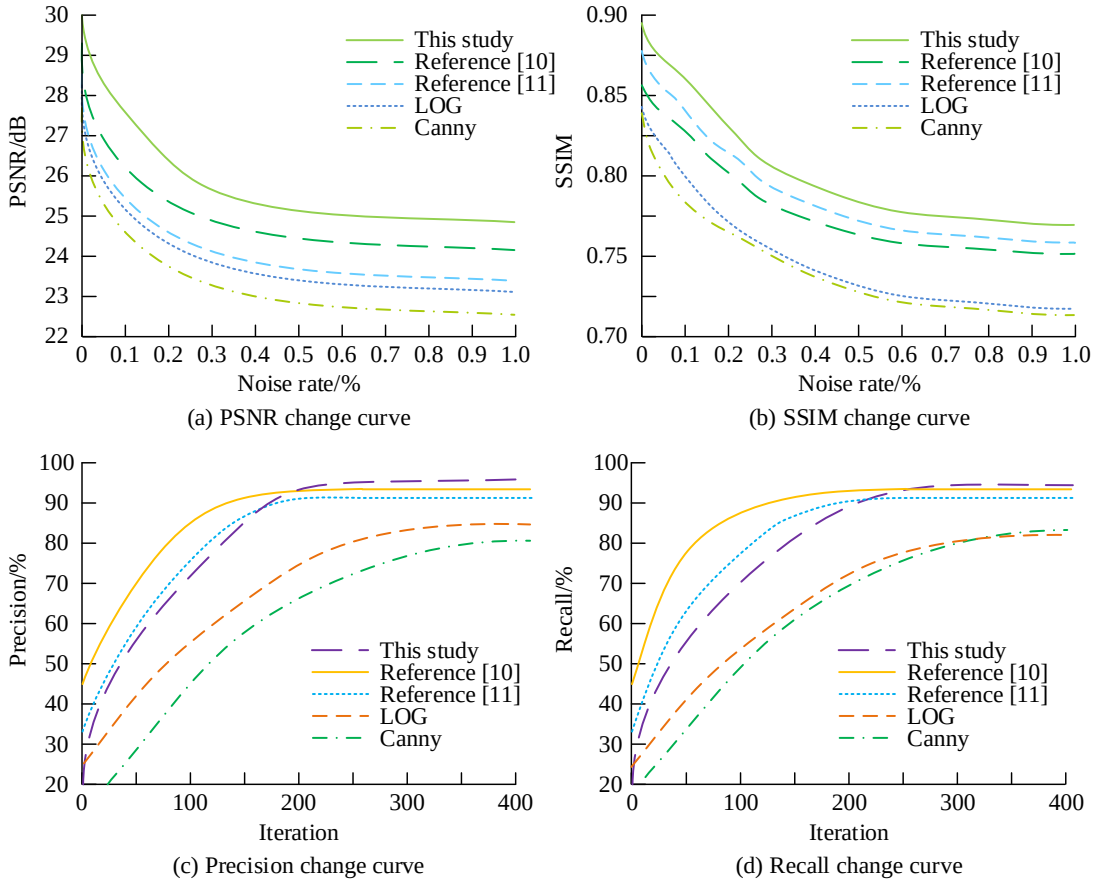

(a) PSNR change curve (b) SSIM change curve

(c) Precision change curve (d) Recall change curve

Figure 10. The variation of the quality of edge images extracted by various methods with the noise level and the training situation

Each method's PSNR immediately drops at the NL below 0.3% in Figure 10(a), after which it gradually and slowly declines. The CA curve is always in the lowest region, indicating that there is significant structural distortion between its edge detection results and the original image. As the NL increases, so does the study methodology. At its highest NL, its PSNR is 24.4389dB, which is consistently greater than that of the other techniques. Whereas, the PSNRs of Zhang et al. [10], Tuo et al. [11], LOG and Canny are 24.15dB, 23.48dB, 23.07dB, and 22.50dB, respectively. This suggests that the method has a lower level of distortion as compared to the other methods, and is more identical to the original images identical to the original image. In Figure 10(b), the proposed method of the study has a higher SSIM compared to the other methods. The SSIM is 0.76 when it is at the maximum NL. This research method effectively addresses the issue of "weak edge loss due to excessive smoothing" in traditional Gaussian filtering. It does so by dynamically adjusting the window size and replacing noise pixels, which have extreme salt-and-pepper characteristics, with the median. It also retains the original values of normal pixels. For instance, under 0.5% noise, traditional Canny generates over 20% pseudo-edges due to salt-pepper noise. The proportion of pseudo-edges in the improved method is less than 5%. Additionally, the gradient domain weighted guided filtering method proposed in the research is a weak edge preservation technique that uses the input image as a guide map. It distinguishes edge areas from flat areas through edge perception constraints. The filtering intensity is reduced in edge areas to retain needle lines and silver wire contours. Meanwhile, the filtering intensity is enhanced in flat areas to suppress Gaussian noise. Although the adaptive bilateral filtering in Tuo et al. [11] performed well with low-texture-complexity clothing patterns, the high texture density of lacquerware patterns (e.g., the multi-line overlap of carvings and fillings) prevents the fixed 5×5 filtering window from accurately distinguishing edges from noise.

Figures 10(c) and Figure 10(d) show the variation of precision and recall of each method with the number of iterations. The improved method increases the precision and recall rapidly and stabilizes with the number of iterations. The optimization is reached after about 200 iterations: 96.21% precision and 94.83% recall. Although the Zhang et al. [10], Tuo et al. [11] methods converge faster than the traditional algorithm, the final accuracy (92.01%, 90.14.%) and recall (93.20%, 90.05%) are still lower than the improved method. The non-maximum suppression of traditional Canny only selects two neighboring pixels for comparison based on the gradient direction, which is prone to losing the "fine edges with smooth gradient direction changes" (such as the arc segments of needle-cut lines). The improved method uses the modulus value of the gradient component to determine the direction of the main gradient. It dynamically selects four neighboring pixels in combination with symbol combinations and calculates the interpolation result using a weight coefficient. This achieves pixel-level edge positioning. Although the genetic algorithm in Zhang et al. [10] can optimize the threshold, it does not improve the non-maximum suppression mechanism. On the arc lines of the silver-carved filamentation, due to the continuous change in the gradient direction, there is still a 12% edge breakpoint. Although the 45°/135° gradient template in Tuo et al. [11] improved oblique edge detection, it significantly deviated from the actual gradient direction at curve turning points, achieving an accuracy rate of only 90.14%.

To further compare the detection performance of the methods, the study counts the number of edge points extracted and the time required for the detection process of the various methods for edge detection on eight lacquerware images. Figure 11(a) shows the number of edge points extracted by each method and Figure 11(b) shows the time required for the detection process.

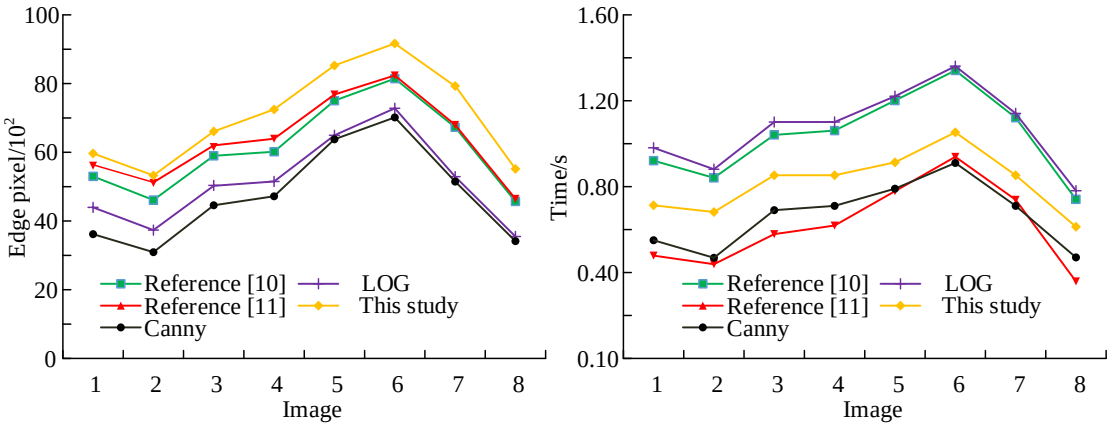

(a) The number of edge pixels extracted by each method

(b) The extraction time of image edge pixels of each method

Figure 11. Each method to detect edge points number and inspection time

In Figure 11(a), the number of edge points extracted by the proposed method of the study is more and the average number of edge band points is 723. The number of edge points extracted by the other compared methods in each image is lower than the research method. The average detection time of the research technique is 0.82 seconds, which is marginally longer than that of the CA and LOG algorithms, as displayed in Figure 11(b). This is because both hybrid filtering and interpolation suppression use "local window calculation and iterative termination condition optimization" (e.g., termination when the cluster center remains unchanged). This balances algorithm performance and computational complexity while avoiding the efficiency issue in Zhang et al. [10] (the genetic algorithm takes a long time to optimize the threshold). In contrast, the Canny and LOG algorithms are less time-consuming, but the completeness of edge point extraction is insufficient. Zhang et al. [10] and Tuo et al. [11] can extract more edge points, but the time consumed increases significantly due to redundant computation, and the average detection time is 0.93s and 0.96s, respectively. The genetic algorithm in Zhang et al. [10] study, requires over 300 iterations to optimize the threshold, resulting in a 21% increase in time consumption. The adaptive bilateral filtering in Tuo et al. [11] has relatively high computational complexity ($O(n^2)$) for the window, which increases time consumption by 17%.

The research introduces a hybrid filtering and adaptive interpolation suppression strategy in the edge detection stage. Although it slightly increases the computational cost, it still has good scalability while maintaining high edge integrity. The experimental platform is based on medium-configuration hardware (Intel i5-7300HQ, 16GB RAM). When used in a high-performance computing cluster or a GPU-accelerated environment, such as one with an RTX 3080 or higher, it can significantly increase processing speed through parallel computing. This makes it ideal for large-scale image processing requirements in museums or industrial applications. In addition, the algorithm's modular design supports distributed processing, making it suitable for digitizing batches of lacquerware cultural relics. The study further determines the binary classification ability of each algorithm by true positive rate (TPR) and true negative rate (TNR). The TPR and TNR of various methods for detecting different images are shown in Figure 12.

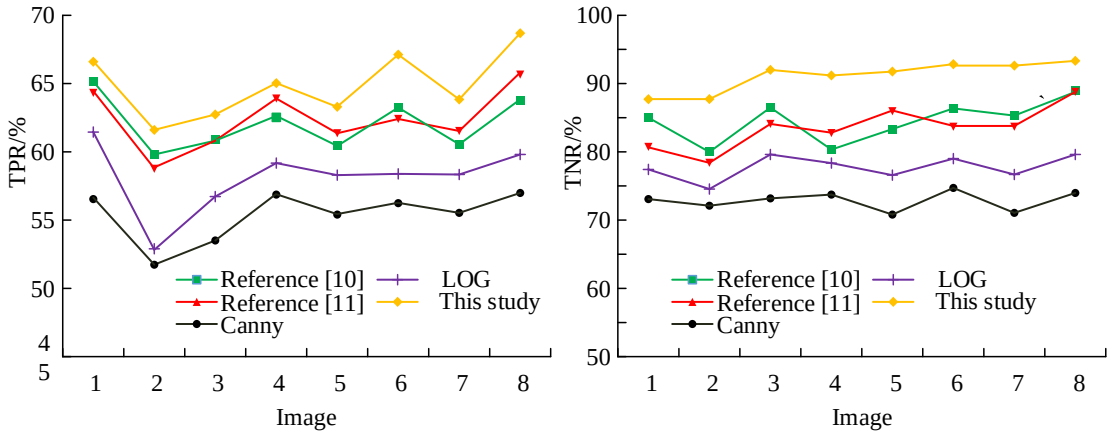

(a) TPR of image edge detection by each algorithm

(b) TNR of image edge detection by each algorithm

Figure 12. The average values of TPR and TNR are compared when different images are detected by each method

In Figure 12(a), the proposed method of the study performs optimally in terms of TPR, with an average TPR of 64.88%, which is higher than the other compared methods. This indicates that the method more effectively captures the presence of edge points, provides greater integrity in edge detection, and recognizes subtle edges in the lacquerware decorative pattern more accurately. In contrast, the CA and the LOG algorithm have lower TPR, reflecting that they do not capture the edges adequately. The TPR of Zhang et al. [10] and [11] is 63.64% and 64.75% respectively, which is still lower than the research method. In Figure 12(b), the TNR of the research method also stays at a high level with an average value of 93.04%. It indicates that it has a lower misclassification rate for non-marginal points and better detection accuracy. This is because hybrid filtering's "gradient domain weighting" makes the distinction between edge and flat areas more precise. Additionally, adaptive interpolation suppression's "multi-neighborhood calculation" reduces the pseudo-edges caused by background noise. The two work together to achieve a balance between high TPR and high TNR, which is crucial for the reconstruction of lacquerware patterns. If the TPR is too low, the line details will be lost. If the TNR is too low, the edges of the patterns will be "rough," failing to meet the "refinement" requirements of traditional lacquerware. The TNR of the methods in the Zhang et al. [10] and Tuo et al. [11] study, is relatively low, with mean values of 84.77% and 85.06%, respectively. The method in Zhang et al. [10] is not optimized for the low-contrast edges of lacquerware (such as the junction of silver-gray and dark gray). Although the TPR reaches 63.64%, the false edge misjudgment rate still reaches 15.23% (TNR 84.77%) under 1.0% noise. The adaptive bilateral filtering in Tuo et al. [11] has insufficient anti-interference ability against high-texture backgrounds (such as multi-color overlapping of carvings and fillings), with a TNR of only 85.06%.

According to the improved K-means++ color extraction and Canny edge detection method, the study further applies it to the practice of lacquerware decorative pattern design to generate the decorative pattern scheme shown in Figure 13. During the design process, the primary colors of needle carving with a pulling knife and silver-thread luster carving (e.g., black, silver-gray, red-brown, etc., as shown in Table 2) are first extracted by improving the K-means++ algorithm. This ensures that the color scheme fits the color ratio and visual characteristics of the traditional crafts. At the same time, the improved CA accurately extracts the edge contour of a typical decorative pattern. It retains the continuity and subtle transitions of the lines and provides an accurate structural basis for reconstructing the pattern. This fusion of traditional craft features and digital design is realized.

Figure 13. Design of lacquerware ornament

In Figure 13, the black base matches the main colors, such as silver gray and red brown, continuing the hierarchical contrast of the traditional process. Other colors can be matched according to demand. The clear and coherent edges of the decorative pattern not only retain the rhythmic sense of the traditional pattern but also enhance its delicacy through accurate edge positioning. This verifies the reliability of the improved algorithm in color restoration and edge extraction. To achieve the transformation of this algorithm into practical application tools for artisans or museums, a three-tier architecture software integration solution can be designed. The bottom layer is the core library of algorithms, which encapsulates improved color clustering and edge detection modules as application programming interfaces (apis). The middle layer is the application service layer. It is responsible for calling the underlying APIs and handling logic such as project management, batch processing, and parameter presetting and adjustment. For example, it presets optimized parameter templates for different processes, such as lacquer carving and painting. The top layer is the interactive interface layer, providing an intuitive visual operation interface for end users (artisans or curators). In the interface design, two core functional modules can be developed: First, the "Intelligent Extraction" module. After users upload images of cultural relics, the system automatically generates the main color palette and clear decorative outline lines. The "Auxiliary Design" module allows users to recreate designs based on extracted colors and outlines. Users can adjust color schemes, fill in new textures, and combine pattern units. The system outputs standard formats (such as SVG vector graphics, PSD layered files) to facilitate seamless integration with commonly used design software (such as Adobe Illustrator).

5. Discussion

The proposed improved K-means++ clustering and Canny edge detection algorithms achieved both accuracy and robustness in the digital extraction of lacquerware color and decorative pattern. The core innovation of it lied in the multi-module collaborative optimization strategy. SVD dimensionality reduction maximized the preservation of a color image's core color information while compressing the data volume by retaining high-energy singular values. This solved the problem of traditional K-means++ being sensitive to initial centers. The secondary clustering strategy further integrated the first round of adaptive primary color collection, and generated a comprehensive color spectrum with a PSNR mean value of 31.47 dB, which was superior to the FCM algorithm of Bhagat et al. [6] (30.02 dB) and the K-mean clustering of Ning et al. [7] (28.37 dB). Especially in the needle carving with a pulling knife process, the color separation accuracy of the black substrate with silver-thread accents was significantly improved (SSIM 0.95). The effectiveness of structured dimensionality reduction and hierarchical clustering in complex color scenes was verified. The combination strategy of hybrid filtering and adaptive interpolation suppression in decorative pattern detection was the key to the performance breakthrough. Adaptive median filtering effectively suppressed pretzel noise through dynamic window adjustment, while bootstrap filtering preserved weak edge details. The synergistic effect of the two resulted in a PSNR of 24.43 dB even at 1.0% NL, which outperformed the genetic algorithm optimized Canny (24.15 dB) in Zhang et al. [10] and the improved Canny (23.48 dB) in Tuo et al. [11]. Adaptive linear interpolation suppression improved the TPR to 64.88% by gradient direction weight assignment, and solved the problem of leakage detection of lacquerware fine-grained edges by traditional algorithms with a TNR of 93.04%. It demonstrated its anti-interference ability in complex texture background. The research introduces adaptive mechanisms in both the clustering and edge detection stages to reduce the reliance on manual parameters. In color clustering, K_1 is dynamically determined through adaptive critical distance to avoid the deviation of artificially setting the number of clusters. K_2 can be flexibly set according to design requirements. Experiments show that within the range of K_2= 8 to 16, both PSNR and SSIM remain at a relatively high level (PSNR>28dB, SSIM>0.91). It indicates that the algorithm has certain robustness to K_1. In edge detection, when the regularization parameter σ of the guided filter fluctuates within the range of 0.005 to 0.02, the variation range of PSNR and TPR is less than 2%. This suggests that the filtering process is not sensitive to parameter changes.

However, the test data of the current study is limited to needle carving with a pulling knife and silver-thread cluster carving. It does not cover multi-material lacquerware, such as painted and inlaid pieces. Additionally, the adaptability of the model to color gradients and material reflections needs to be verified. Future research can be carried out in three aspects: constructing a cross-craft lacquerware dataset to enhance the generalization ability, introducing an adaptive clustering number determination mechanism to improve the automation level of the algorithm, and exploring a lightweight network architecture to optimize the detection efficiency. The research introduces a new approach to digitally conserving cultural relics by combining traditional craftsmanship with modern computer vision. Its technical framework can be applied to reconstructing patterns and designing innovations in other fields of cultural relics, such as ceramics and embroidery. For ceramics with high surface gloss, a mirror reflection suppression pretreatment step should be added, and clustering should be prioritized in the Lab color space with uniform perception to improve the accuracy of glaze color extraction. For textiles, their patterns often have periodic unit structures. After edge extraction, texture feature analysis, such as Gabor filters, can be introduced to identify pattern units. Image correction can also be carried out while considering the fabric deformation factor. For metal objects with weak contrast between the pattern and the base, the excellent edge protection characteristics of this method can be utilized. Focusing on optimizing the gradient calculation and adaptive threshold mechanism enhances the detection rate of weak edges, such as scratches and inlays.

6. Conclusion

The study proposed a digital design method for lacquerware colors and decorative patterns. This method was based on improved K-means++ clustering and Canny edge detection. Through SVD dimensionality reduction and quadratic clustering, it optimized the color extraction process, solving the problem of initial center sensitivity in traditional algorithms. This allowed for the accurate separation of main colors in lacquerware with complex craftsmanship, such as needle carving with a pulling knife and silver-thread luster carving. It also accurately restored the proportionality between black bases and accent colors, such as silver-gray and red-brown. This was a key detail in preserving the characteristics of traditional crafts. For decorative pattern edge detection, the method integrated hybrid filtering (adaptive median filtering and bootstrap filtering) and adaptive interpolation suppression technology. This combination improved the integrity and anti-interference ability of edge detection while effectively retaining the continuity and subtle transitions of pattern lines, which were critical to lacquerware's artistic expression. Experimental verification showed the method achieved high and stable performance: In color extraction, it achieved a mean PSNR of 31.47 dB and an SSIM of 0.95 when extracting 16 feature colors. It maintained a PSNR of 28.83 dB when extracting only eight feature colors. In edge detection, it achieved a PSNR of 24.43 dB at a NL of 1.0%, with 64.88% sensitivity and 93.04% specificity. This outperformed comparison methods such as traditional FCM, original K-means++, and conventional Canny. This method provides technical support for the digital preservation of traditional lacquerware craftsmanship. Its multi-module, synergistic optimization strategy combines dimensionality reduction, clustering, filtering, and interpolation. This strategy can be extended to digital pattern reconstruction for other cultural relics, such as ceramics and embroidery. This extension promotes the in-depth integration and innovative development of traditional art forms with modern computer vision technology.

7. Declarations

7.1. Author Contributions

Conceptualization, W.P. and B.H.; methodology, W.P. and B.H.; validation, B.H.; formal analysis, W.P.; investigation, B. H.; data curation, W.P.; writing—original draft preparation, W.P. and B.H.; writing—review and editing, W.P. and B.H. All authors have read and agreed to the published version of the manuscript.

7.2. Data Availability Statement

The data presented in this study are available on request from the corresponding author.

7.3. Funding

The authors received no financial support for the research, authorship, and/or publication of this article.

7.4. Institutional Review Board Statement

Not applicable.

7.5. Informed Consent Statement

Not applicable.

7.6. Declaration of Competing Interest

The authors declare that they have no known competing financial interests or personal relationships that could have appeared to influence the work reported in this paper.

8. References

[1] Xinying, H., Yufan, Z., Xin, W., & Tong, T. (2023). Micro - destructive detection of a Southern Song lacquerware fragment and study of its lacquering techniques. Sciences of Conservation and Archaeology, 35(2), 116–124. doi:10.16334/j.cnki.cn31-1652/k.20210902243.

[2] Zhang, G., Wang, Z., Xia, J., & Wang, N. (2025). Species identification of the cores of wooden lacquerwares excavated from the lower reaches of Yangtze River and research on the development of their fabrication processes. Sciences of Conservation and Archaeology, 37(2), 167–178. doi:10.16334/j.cnki.cn31-1652/k.20231103102.

[3] Zhang, X., & Dolah, J. (2024). Research on Animal and Plant Patterns of Pingyao Lacquerware in the Ming and Qing Dynasties. Herança, 7(3), 157–164. doi:10.52152/heranca.v7i3.767.

[4] Zhang, T., & Deng, C. (2024). Technical Repair Method of Poyang Bodiless Lacquerware Based on Scale-Invariant Feature Transform Algorithm for Healthcare Vision. Journal of Testing and Evaluation, 52(1), 315–326. doi:10.1520/JTE20210460.

[5] Habiban, M., Hamade, F. R., & Mohsin, N. A. (2024). Hybrid Edge Detection Methods in Image Steganography for High Embedding Capacity. Cybernetics and Information Technologies, 24(1), 157–170. doi:10.2478/cait-2024-0009.

[6] Bhagat, S., Budhiraja, S., & Agrawal, S. (2024). Pattern-based feature set for efficient segmentation of color images using modified FCM clustering. Signal, Image and Video Processing, 18(11), 7671–7687. doi:10.1007/s11760-024-03419-3.

[7] Ning, X., Wu, N., Zhang, R., Chen, T., Jiang, Y., & Jiang, H. (2024). Tenglong Yuan blue and white texture extraction method based on adaptive gamma correction and K-means clustering segmentation coupled algorithm. Journal of the Australian Ceramic Society, 60(1), 1–11. doi:10.1007/s41779-023-00981-w.

[8] Qian, Q., Zheng, Z., Liang, Z., Wu, P., & Du, P. (2023). Application of Semi-Supervised Clustering Algorithm Based on Color Feature to Corrosion Level Identification for Copper. Corrosion and Protection, 44(5), 34–40. doi:10.11973/fsyfh-202305007.

[9] Hasanlou, E., Shams Nateri, A., & Izadan, H. (2024). Fabric colour measurement in the small region of CIELab colour space using a scanner-based subtractive clustering fuzzy inference system. Coloration Technology, 140(5), 782–792. doi:10.1111/cote.12739.

[10] Zhang, Y., Zhang, J., & Qi, L. (2024). Research on the extraction method of woven and embroidered artifacts' patterns based on genetic algorithm optimization of Canny operator. Journal of Silk, 61(6), 1–12. doi:10.3969/j.issn.1001-7003.2024.06.001.

[11] Tuo, W., Du, C., Chen, Q., Wu, C., Wei, X., Zhang, X., & Liu, S. (2024). Clothing pattern contour extraction based on computer vision and Canny algorithm. Fangzhi Xuebao/Journal of Textile Research, 45(5), 174–182. doi:10.13475/j.fzxb.20230502901.

[12] Shi, X., Xu, Z., Cui, L., Zhao, X., & Zhang, W. (2025). ViCo: Human visual perception-based contour extraction of Chinese Tang dynasty textile patterns. Textile Research Journal, 95(9–10), 1169–1183. doi:10.1177/00405175241268771.

[13] Yadav, N., Singh, V., Rani, A., & Goyal, S. (2023). Local Diagonal Maxima-Minima Pattern-based Edge Detection Technique for Ultrasound and Digital Radiography Images. IETE Journal of Research, 69(6), 3211–3221. doi:10.1080/03772063.2021.1912652.

[14] Sabha, M., & Saffarini, M. (2024). Selecting optimal k for K-means in image segmentation using GLCM. Multimedia Tools and Applications, 83(18), 55587–55603. doi:10.1007/s11042-023-17615-9.

[15] Dhal, K. G., Das, A., Sasmal, B., Ray, S., Rai, R., & Garai, A. (2024). Fuzzy C-Means for image segmentation: challenges and solutions. Multimedia Tools and Applications, 83(9), 27935–27971. doi:10.1007/s11042-023-16569-2.

[16] Rahman, M. M., Islam, M. R., Afjal, M. I., Marjan, M. A., Uddin, M. P., & Islam, M. M. (2025). Segmentation-based truncated-SVD for effective feature extraction in hyperspectral image classification. International Journal of Remote Sensing, 46(2), 538–574. doi:10.1080/01431161.2024.2421934.

[17] Niu, P., Wang, F., & Wang, X. (2024). SVD-UDWT Difference Domain Statistical Image Watermarking Using Vector Alpha Skew Gaussian Distribution. Circuits, Systems, and Signal Processing, 43(1), 224–263. doi:10.1007/s00034-023-02460-w.

[18] Li, N., Qi, W., Jiao, J., Li, A., Li, L., & Xu, W. (2024). SPCC: A superpixel and color clustering based camouflage assessment. Multimedia Tools and Applications, 83(9), 26255–26279. doi:10.1007/s11042-023-16425-3.

[19] Gijsenij, A., Vazirian, M., Spiers, P., Westland, S., & Koeckhoven, P. (2023). Determining key colors from a design perspective using dE-means color clustering. Color Research and Application, 48(1), 69–87. doi:10.1002/col.22817.

[20] Purohit, J., & Dave, R. (2023). Leveraging Deep Learning Techniques to Obtain Efficacious Segmentation Results. Archives of Advanced Engineering Science, 1(1), 11–26. doi:10.47852/bonviewaaes32021220.

[21] Lu, H., Mao, H., Zhou, H., Zhen, B., Zhong, Y., & Yang, B. (2025). Applying Canny edge detection and Hough transform algorithms to identify irrigation channel boundaries in irrigation districts. Journal of Irrigation and Drainage, 44(5), 47–56. doi:10.13522/j.cnki.ggps.2024375.

[22] Liu, L., Liu, Z., Hou, A., Qian, X., & Wang, H. (2024). Adaptive edge detection of rebar thread head image based on improved Canny operator. IET Image Processing, 18(5), 1145–1160. doi:10.1049/ipr2.13015.

[23] Wang, H., Peng, H., Tang, Y., Guan, Y., Liang, Y., Wang, L., Zhao, Y., Wang, X., Gao, R., & Huang, H. (2024). Portable Structure Surface Crack Detection System Based on Android Platform. Wuhan University Journal of Natural Sciences, 29(2), 154–164. doi:10.1051/wujns/2024292154.

[24] Ranjan, R., & Avasthi, V. (2023). Edge Detection Using Guided Sobel Image Filtering. Wireless Personal Communications, 132(1), 651–677. doi:10.1007/s11277-023-10628-5.

[25] He, L., Xie, Y., Xie, S., Jiang, Z., & Chen, Z. (2024). Iterative Self-Guided Image Filtering. IEEE Transactions on Circuits and Systems for Video Technology, 34(8), 7537–7549. doi:10.1109/TCSVT.2024.3374758.

[26] Zhou, W. (2023). Image Dehazing Enhancement Algorithm Based on Mean Guided Filtering. Journal of Information Processing Systems, 19(4), 417–426. doi:10.3745/JIPS.02.0195.

[27] Riyono, J., Pujiastuti, C. E., Puspa, S. D., Supriyadi, & Putri, F. N. R. (2024). Enchancing Lung Disease Classification through K-Means Clustering, Chan-Vese Segmentation, and Canny Edge Detection on X-Ray Segmented Images. Jurnal Online Informatika, 9(1), 89–99. doi:10.15575/join.v9i1.1178.

[28] Ravendran, A., & Rianmora, S. (2021). Application of image-based acquisition techniques for additive manufacturing using canny edge detection. Journal of Computational and Applied Research in Mechanical Engineering, 10(2), 391–404. doi:10.22061/jcarme.2019.4355.1524.

[29] Salunke, D., Tekade, P., Ranjan, N., Ujalambkar, D., Sangve, S., & Mane, D. (2023). Real-Time Dimension Detection using Customized Canny Edge Detection Algorithm. International Journal of Engineering Trends and Technology, 71(9), 375–384. doi:10.14445/22315381/IJETT-V71I9P233.

[30] Wang, W., Liu, Y., Xiao, L., Fang, J., Wang, J., & Wang, J. (2023). Research on digitalization of ancient Shu Brocade patterns based on improved generative adversal network and vector rendering technology. Journal of Silk, 60(11), 18–27. doi:10.3969/j.issn.1001-7003.2023.11.003.